

On the structure of Small Magellanic Cloud star clusters

Andrés E. Piatti^{1,2*}

¹ Instituto Interdisciplinario de Ciencias Básicas (ICB), CONICET-UNCUYO, Padre J. Contreras 1300, M5502JMA, Mendoza, Argentina;

² Consejo Nacional de Investigaciones Científicas y Técnicas (CONICET), Godoy Cruz 2290, C1425FQB, Buenos Aires, Argentina

Received / Accepted

ABSTRACT

It has been recently shown from observational data sets the variation of structural parameters and internal dynamical evolution of star clusters in the Milky Way and in the Large Magellanic Cloud (LMC), caused by the different gravitational field strengths that they experience. We report here some hints for such a differential tidal effects in structural parameters of star clusters in the Small Magellanic Cloud (SMC), which is nearly 10 times less massive than the LMC. A key contribution to this study is the consideration of the SMC as a triaxial spheroid, from which we estimate the deprojected distances to the SMC center of the statistically significant sample of star clusters analyzed. By adopting a 3D geometry of the SMC, we avoid the spurious effects caused by considering that a star cluster observed along the line-of-sight is close to the galaxy center. When inspecting the relationships between the star cluster sizes (represented by the 90% light radii), their eccentricities, masses and ages with the deprojected distances, we find: (i) the star cluster sizes are not visibly affected by tidal effects, because relatively small and large objects are spread through the SMC body. (ii) Star clusters with large eccentricities (≥ 0.4) are preferentially found located at deprojected distances smaller than ~ 7 -8 kpc, although many star clusters with smaller eccentricities are also found occupying a similar volume. (iii) Star clusters more massive than $\log(M/M_{\text{dot}}) \sim 4.0$ are among the oldest star clusters, generally placed in the outermost SMC region and with a relative small level of flattening. These findings contrast with the more elongated, generally younger, less massive and innermost star clusters.

Key words. Methods: observational - Galaxies: Magellanic Clouds - Galaxies: star clusters: general

* e-mail: andres.piatti@unc.edu.ar

1. Introduction

The structure of star clusters evolves over their lifetime, mainly because of the stellar evolution, two-body relaxation and tidal effects caused by the host galaxy's gravitational field (e.g., Heggie & Hut 2003; Lamers et al. 2005; Kruijssen & Mieske 2009; Gieles et al. 2011; Webb et al. 2013, 2014; Shukirgaliyev et al. 2018). Although mass loss due to tidal heating has long been treated theoretically and from numerical simulations (e.g., Gnedin et al. 1999; Baumgardt & Makino 2003; Gieles et al. 2006; Lamers & Gieles 2006; Gieles & Baumgardt 2008; Kruijssen et al. 2011; Gieles & Renaud 2016), the magnitude of this phenomenon on different star clusters has been more difficult to measure. Indeed, the observed variation across the body of a galaxy of the core, half-mass, and Jacobi radii, cluster eccentricity, half-mass relaxation time, cluster mass, among other star cluster parameters, has relatively recently been studied in some limited number of cases.

Piatti et al. (2019) analyzed the extent in shaping the structural parameters and internal dynamics of the globular cluster population caused by the effects of the Milky Way gravitational field. They employed a homogeneous, up-to-date data set with kinematics, structural properties, current and initial masses of 156 globular clusters, and found that, in overall terms, cluster radii increase as the Milky Way potential weakens. Core radii increase at the lowest rate, while Jacobi radii do at the fastest one, which implies that the innermost regions of globular clusters are less sensitive to changes in the tidal forces with the Galactocentric distance. The Milky Way gravitational field also differentially accelerates the internal dynamical evolution of globular clusters, with those toward the bulge appearing dynamically older. Globular clusters with large orbital eccentricities and inclination angles experience a higher mass loss because of more tidal shocks at perigalacticon and during disc crossings (Piatti 2019).

Milky Way open clusters are also subject to tidal heating. Because they are younger than globular clusters, mass loss due to stellar evolution can be more important, particularly if they are younger than few hundred million years, while two-body relaxation becomes important as the mass loss rate due to stellar evolution continues to decrease (Lamers et al. 2005). Nevertheless, shocks with giant molecular clouds are known to be the dominant source of mass-loss over the open cluster's lifetime (Lamers & Gieles 2006). Joshi et al. (2016) studied a statistically complete sample of open clusters located within 1.8 kpc from the Sun and found that their present-day masses follow a linear relationship with their respective ages. Assuming that the gravitational field does not vary significantly within such a circle, stellar evolution could be responsible for such a trend.

The Large Magellanic Cloud (LMC) is nearly 10 times less massive than the Milky Way (Deason et al. 2020) and differential tidal effects are also seen within its population of globular clusters. Piatti & Mackey (2018) built extended stellar density and/or surface brightness radial profiles for almost all the known LMC globular clusters and found that those located closer than ~ 5 kpc from the LMC center contain an excess of stars in their outermost regions with respect to the stellar density expected from a King profile, which are not seen in globular clusters located beyond ~ 5 kpc from the LMC center. In addition, globular cluster sizes show a clear dependence with their posi-

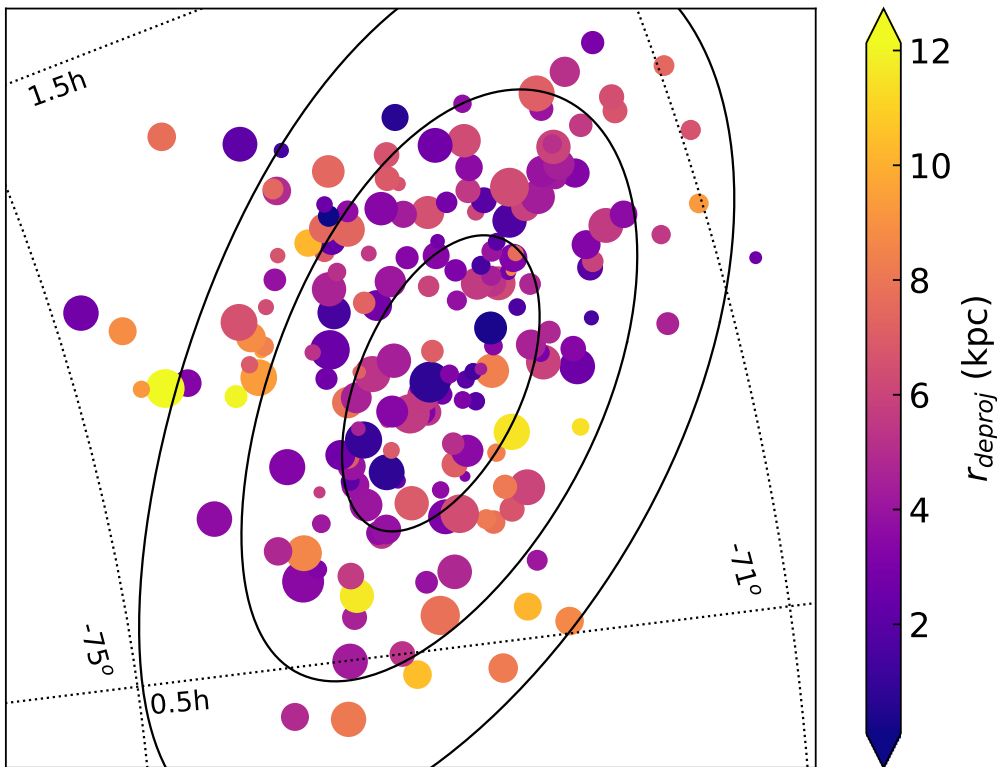


Fig. 1. Equal-area Hammer projection of the SMC in equatorial coordinates. Three ellipses with semi-major axes of 1° , 2° , and 3° are superimposed. Symbols are colored according to the star cluster distance to the SMC center, while their sizes are proportional to the star cluster 90% light radii.

tions in the galaxy, in the sense that the closer the globular cluster to the LMC center, the smaller its size. Although the masses of the LMC globular clusters are commensurate, the outermost regions of globular clusters located closer than ~ 5 kpc from the LMC center seem to have dynamically evolved faster. Having the globular clusters orbited the LMC at different mean distances from its center along their lifetime, the distinction of their structural properties reflect the differential tidal effects between them.

We wonder whether tidal heating still has an important role in the structural parameters of star clusters in galaxies less massive than the LMC. We focus here on the Small Magellanic Cloud, which is nearly 10 times less massive than the LMC (van der Marel & Kallivayalil 2014; Stanimirović et al. 2004), because it has a statistically complete sample of studied star clusters to explore this issue. Gieles et al. (2007) analyzed a sample of 195 star clusters in the SMC and found no evidence for cluster tidal dissolution in the first gigayear. They arrived to this conclusion by comparing the observed star cluster frequency with that predicted by stellar evolutionary models, assuming no tidal dissolution.

The paper is organized as follows. In Section 2 we present the data set used and different star cluster parameters obtained from it. Section 3 deals with the analysis of the variation of structural parameters as a function the star cluster distance to the SMC center. Finally, Section 4 summarizes the main results of this work.

2. SMC star cluster properties

We gathered information from two main sources: the recent catalog of star clusters compiled by Bica et al. (2020), from which we retrieved star cluster ages; and Table 2 of Hill & Zaritsky (2006), from which we used star cluster coordinates (RA and Dec), 90% light radii (r_{90}), integrated V magnitudes, and cluster eccentricities (ϵ). We would like to note that different SMC imaging surveys have been carried out since the Magellanic Clouds Photometric Survey (Zaritsky et al. 2002) used by Hill & Zaritsky (2006), e.g., VMC (Cioni et al. 2011), OGLE (Udalski et al. 2015), SMASH (Nidever et al. 2017), VISCACHA (Maia et al. 2019), among others. As far as we are aware, none of these surveys have been exploited yet in order to update the parameters derived and analysis done by Hill & Zaritsky (2006), which justifies our choice. We computed the cluster masses using the relationships obtained by Maia et al. (2014, equation 4) as follows:

$$\log(M/M_{\odot}) = a + b \times \log(\text{age}/\text{yr}) - 0.4 \times (M_V - M_{V_{\odot}})$$

with $a = 5.87 \pm 0.07$, $b = 0.608 \pm 0.008$ for a representative SMC overall metallicity $Z = 0.004$ (Piatti & Geisler 2013); $M_{V_{\odot}} = 4.83$. Typical uncertainties turned out to be $\sigma(\log(M/M_{\odot})) \approx 0.2$. We note that the assumption of a single average metallicity for all star clusters does not affect their calculated masses, since metallicity differences imply mass values that are within the uncertainties (see figures 10 and 11 in Maia et al. 2014). We checked that our cluster masses are in very good agreement with those calculated by Hill & Zaritsky (2006, see their figure 16). As for the completeness of the present star cluster sample, we refer the reader to the work by Gieles et al. (2007), which shows that the sample is magnitude limited.

As far as we are aware, the frequent geometry considered to analyze the spatial distributions of SMC star clusters is the elliptical framework proposed by Piatti et al. (2007) as a simple representation of the orientation, dimension and shape of the SMC main body. This framework does not consider the SMC depth, which is much more extended than the size of the galaxy projected in the sky (Ripepi et al. 2017; Muraveva et al. 2018; Graczyk et al. 2020). In an attempt to represent the SMC main body more realistically, we devised a 3D geometry, considering the SMC as an ellipsoid, as follows:

$$\frac{x^2}{a^2} + \frac{y^2}{b^2} + \frac{z^2}{c^2} = 1, \quad (1)$$

where x and y directions are along the semi-minor and semi-major axes in the Piatti et al. (2007)'s framework, respectively, and the z axis is along the line-of-sight. The SMC center is adopted as the origin of this framework, i.e., $(\text{RA}_{SMC}, \text{Dec}_{SMC}) = (13^{\circ}1875, -72^{\circ}8286)$ (Piatti et al. 2007). The projected ellipses in the sky have a position angle $\text{PA}_{SMC} = 54^{\circ}$ and a a/b ratio of 1/2.

The PAs of the star clusters in this rotated coordinate system were calculated using the `positionAngle` routine from `PyAstronomy`¹ (PyA, Czesla et al. 2019), and the observed distances in the sky to the SMC center in R.A. (x_0) and Dec. (y_0), respectively, as follows:

$$x_0 = -(\text{RA} - \text{RA}_{\text{SMC}}) \cos(\text{Dec}) \cos(\text{PA}_{\text{SMC}}) + (\text{Dec} - \text{Dec}_{\text{SMC}}) \sin(\text{PA}_{\text{SMC}}),$$

$$y_0 = (\text{RA} - \text{RA}_{\text{SMC}}) \cos(\text{Dec}) \sin(\text{PA}_{\text{SMC}}) + (\text{Dec} - \text{Dec}_{\text{SMC}}) \cos(\text{PA}_{\text{SMC}}).$$

We assumed that the spatial star cluster distribution is a function of their ages (see figure 8 in Bica et al. 2020, and references therein), so that each ellipsoid corresponds to a fixed age. Using the age gradient of figure 8 in Bica et al. (2020), we entered the star clusters' ages to estimate their corresponding semi-major axis. We additionally used a mean SMC distance of 62.5 kpc (Graczyk et al. 2020), and an average b/c ratio of 1:2.3 (Ripepi et al. 2017; Muraveva et al. 2018; Graczyk et al. 2020, and references therein) to find the projected distance $r = (x^2 + y^2)^{1/2}$ and z values for which:

$$(1 + 3 \times \sin^2(\text{PA})) \times (r/b)^2 + 5.29 \times (z/b)^2 - 1 = 0, \quad (2)$$

where b (kpc) = $1.67 \times \log(\text{age}/\text{yr}) - 10.85$ (age $\lesssim 5$ Gyr) with a dispersion of 0.25 kpc representing the 95% confidence interval of the fitted parameters (figure 8 in Bica et al. 2020). Eq. (2) comes from eq. (1), $x = r \times \sin(\text{PA})$, $y = r \times \cos(\text{PA})$, $a/b = 1/2$ and $b/c = 1/2.3$. We note that if we do not consider the SMC depth ($z=0$), then $x = x_0$ and $y = y_0$. The r and z values that comply with eq. (2) for each star cluster were obtained by evaluating eq. (2) 17600 times, from a grid of values of r from 0.0 up to 11.0 kpc, in steps of 0.1 kpc, and z from 0.0 up to 16.0 kpc, in steps of 0.1 kpc, and then looking for the r and z ones which correspond to the smallest of the 17600 absolute values of eq. (2), which were always smaller than 0.01. We note that, theoretically speaking, the resulting r and z value should lead eq. (2) to be equal to zero. Finally, the linear distance of a star cluster to the SMC center is calculated as $r_{\text{deproj}} = (r^2 + z^2)^{1/2}$. We estimated the uncertainties in r_{deproj} by performing the procedure described above for 1000 realizations with b values randomly chosen in the interval $[b - \sigma(b), b + \sigma(b)]$. Then, we adopted $\sigma(r_{\text{deproj}}) = 1/2.355$ times the $FWHM$ of the r_{deproj} distributions, which resulted to be typically ≈ 1 kpc. Figure 1 illustrates the projected spatial distribution of the star cluster sample where the different deprojected distances to the SMC center are revealed. Some star clusters projected close to the SMC center are relatively distance objects, while others apparently placed in the outer galaxy regions turned out to be closer to the SMC center.

The analysis of the variation of star cluster structural parameters as a function of their deprojected distances to the SMC center supersedes previous ones, which are based on the star cluster

¹ <https://github.com/sczesla/PyAstronomy>

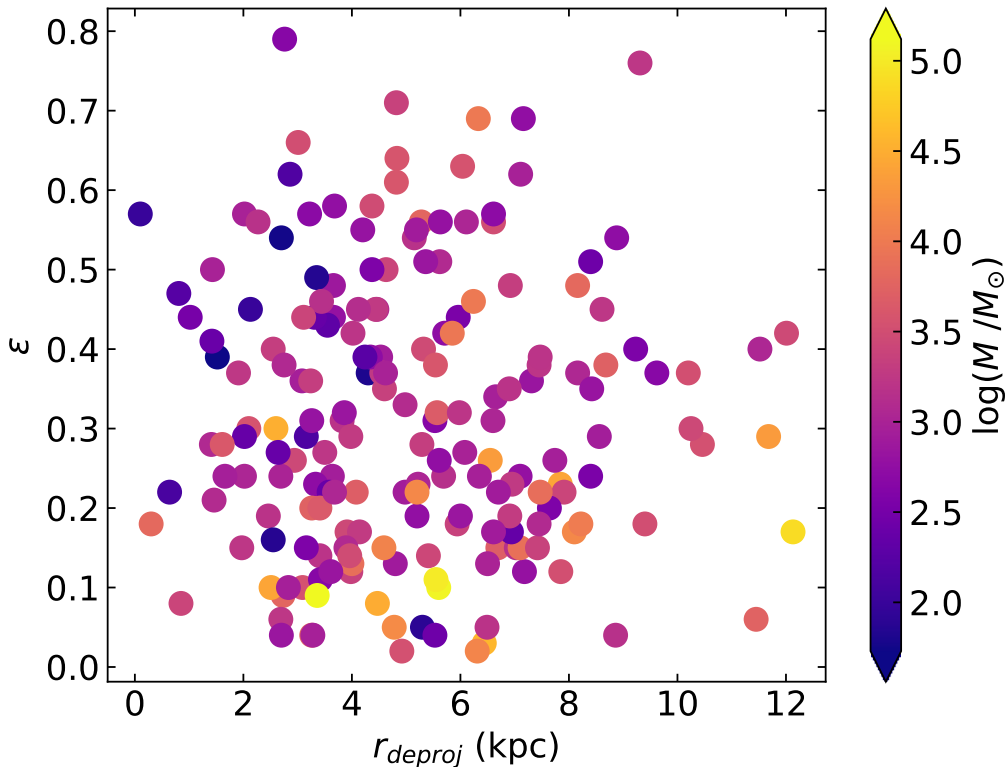


Fig. 2. Star cluster eccentricity versus deprojected distance from the SMC center, color-coded according to the star cluster mass.

positions projected on the sky. As far as we are aware, there are very few SMC star clusters with independent distance estimates (see, e.g. Glatt et al. 2008; Dias et al. 2016). In general, a mean SMC distance modulus is adopted when fitting theoretical isochrones to the CMD of a star cluster, since changes in the distance modulus by an amount equivalent to the average SMC depth leads to a smaller age difference than that resulting from the isochrones (characterized by the same metallicity) bracketing the observed star cluster features in the CMD. Nevertheless, there is still differences between individual star cluster estimates. Glatt et al. (2008) estimated distances for NGC 121, Lindsay 1 and Kron 3 of 64.9 ± 1.2 kpc, 56.9 ± 1.0 kpc and 60.4 ± 1.1 , respectively. However, Crowl et al. (2001) obtained 59.6 ± 1.8 kpc, 53.2 ± 0.9 kpc and 56.7 ± 1.9 kpc, respectively.

3. Analysis and discussion

The different gravitational field strengths experienced by star clusters affect their structural parameters, and ultimately their internal dynamical evolutionary stages. For example, the increase of core, half-mass, and Jacobi radii as a function of the star cluster distance from the Milky Way center was predicted theoretically by Hurley & Mackey (2010) and Bianchini et al. (2015), among others. Star clusters in weaker tidal fields, like those located in the outermost regions of the Milky Way can expand naturally, while those immersed in stronger tidal fields (e.g. the Milky Way bulge) do not. We here use the calculated deprojected distances as a proxy of the SMC gravitational field, to investigate whether some star cluster properties show any trend with it.

Figure 2 shows the eccentricity versus deprojected distance plane for the studied star cluster sample, from which some obvious features arise at a glance. The eccentricities span a wide range of values ($0.0 < \epsilon < 0.8$) for deprojected distances $\lesssim 7$ -8 kpc from the SMC center. For larger deprojected distances, they span a significantly narrower range ($0.0 < \epsilon \lesssim 0.4$). This behavior seems to be independent of the star cluster size, because relatively small and large objects are located throughout the whole covered SMC body (see Fig. 3). The morphology of star clusters can be shaped by different mechanisms, such as dynamical relaxation and decay of initial velocity anisotropy, cluster rotation, external perturbations, differential interstellar extinction, etc (see Chen & Chen 2010, for a review). Milky Way globular clusters have a median eccentricity of ~ 0.13 , with those close to the galaxy bulge having various degrees of flattening, in comparison with those away from the Galactic center that tend to be spherical. In the LMC, the globular cluster population shows evidence for radial variation of the cluster eccentricity (Kontizas et al. 1989), while in the SMC Hill & Zaritsky (2006) find that the eccentricity of star clusters correlates with their masses more strongly than with their ages. Figure 2 reveals that the correlation of the eccentricity with the star cluster mass is not apparent, because star clusters less massive than $\log(M/M_{\odot}) \sim 4.0$ are distributed at any eccentricity. However, there is a hint for more massive star clusters to have in general terms eccentricities smaller than 0.4. This would make massive SMC star clusters to belong to a distinct group of objects.

The two different eccentricity regimes mentioned above (for r_{deproj} smaller or larger than ~ 7 -8 kpc) would also seem to be a distinguished feature. We note here that because of the existence of an age gradient, these two eccentricity regimes could hide an eccentricity-age dependence.

The trend of star cluster ages with the deprojected distances is observed in Fig. 3, where some correlation arises, in the sense that the older the star cluster the farther its location to the SMC center. However, the oldest star clusters are not the most distant ones to the SMC center, but somehow located at the midst of the deprojected distance range, where young star clusters are also seen. Such a mixture of star cluster ages along the deprojected distances is caused by the spheroidal geometry adopted to map more tightly the observed SMC structure and star cluster age gradient. For example, the plane $z = 0.0$ kpc contains old star clusters (the outermost ones in the plane of the sky), that are located comparatively closer to the SMC center than younger star clusters observed along the line-of-sight.

Star clusters with eccentricities larger than ~ 0.4 nearly span the whole age range, as those with smaller eccentricities do (see also Fig. 4). This is visible from the inspection of Fig. 3 for deprojected distances smaller than ~ 7 -8 kpc. Therefore, an eccentricity-age dependence does not find any support. This result is not in opposition with the fact that star clusters with eccentricities smaller than ~ 0.4 and located at deprojected distances larger than ~ 7 -8 kpc are among the old SMC star clusters. It would seem that there is a group of massive and old star clusters located in the outermost SMC regions with relatively small eccentricities, rather than a correlation of the eccentricity with the star cluster mass and age,

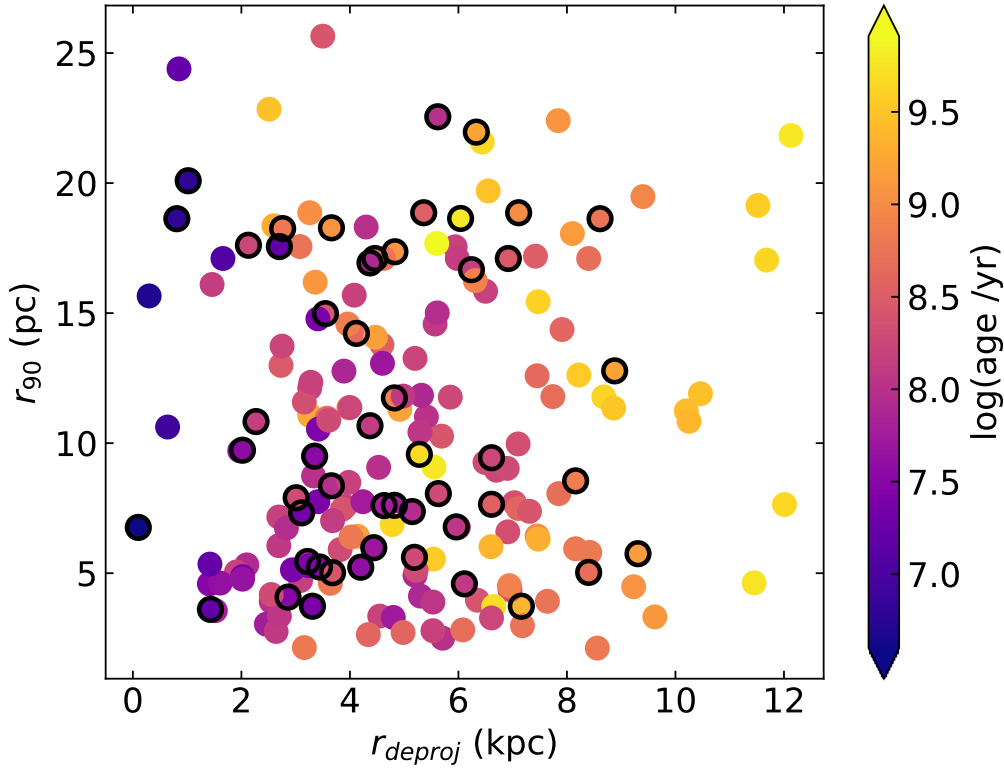


Fig. 3. Star cluster size (r_{90}) versus deprojected distance from the SMC center, color-coded according to their ages. Star clusters with $\epsilon > 0.4$ are highlighted with black open circles.

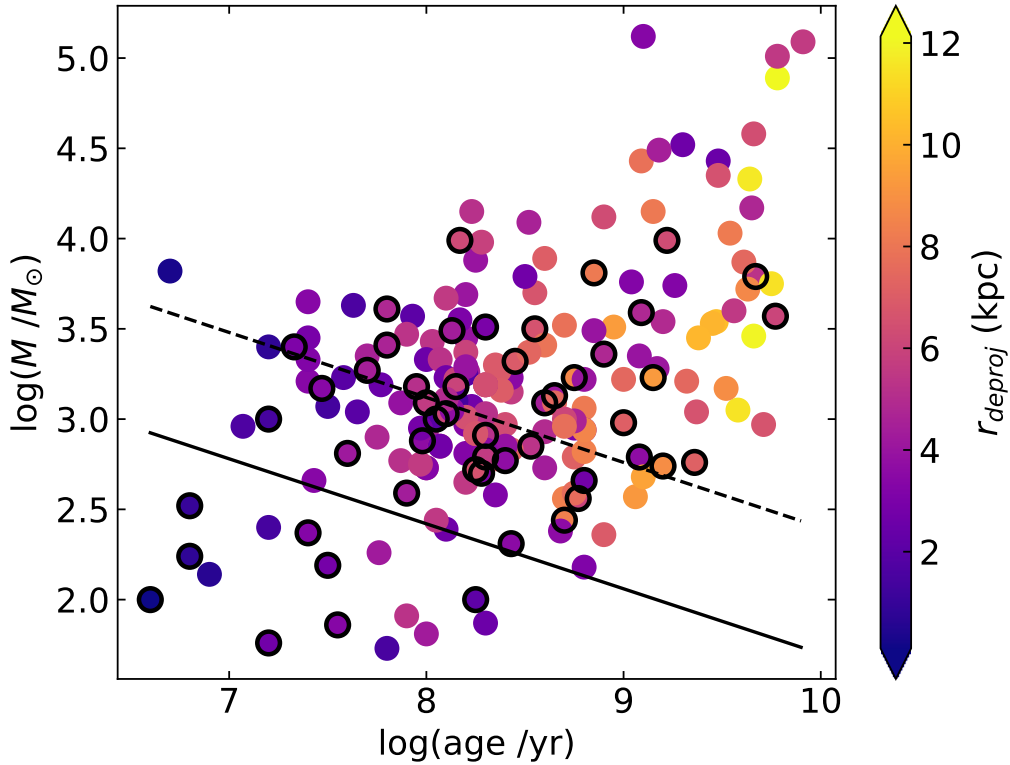


Fig. 4. Star cluster mass versus deprojected distance from the SMC center, color-coded according to their deprojected distances from the SMC center. Star clusters with $\epsilon > 0.4$ are highlighted with black open circles. The straight solid line is the relationship found by Joshi et al. (2016) for Milky Way open clusters located within 1.8 kpc from the Sun, while the dashed and dotted ones are parallel ones to that of Joshi et al. (2016) drawn for comparison purposes (see text for details).

Figure 3 also tells us that the star cluster sizes do not show any correlation with the deprojected distances, i.e., they would not be affected by the SMC gravitation field, as it is the case of Milky Way and LMC globular clusters (Piatti & Mackey 2018; Piatti et al. 2019), which are bigger as they are located further from the galaxy center. This finding puts a limit to the galaxy mass, a value in between the LMC and the SMC mass, in order to the galaxy gravitational field can drive the size of its star clusters. We point out that old globular clusters in the Milky Way and the LMC are on average one order of magnitude more massive than massive SMC star clusters (Piatti & Mackey 2018), so that the comparison between them could favor a minimum galaxy mass more similar to that of the LMC. This also could have its own impact in the computation of the cluster mass lost by tidal disruption along the entire lifetime of star clusters stripped off the SMC by the LMC (Carpintero et al. 2013). In the standard cosmological scenario (Moore et al. 1999; D’Onghia & Lake 2008), accreted globular clusters are formed in small dwarf galaxies. Hence, most of the cluster mass lost by tidal disruption should have disrupted once the star cluster is under the effects of the Milky Way gravitational field, because low mass galaxies would not seem to affect seriously the mass budget of its massive globular clusters. Nevertheless, the large eccentricity values found only in SMC star clusters located inside a volume of radius $\sim 7\text{-}8$ kpc, implies some kind of distortion that might be caused by the SMC tidal forces. At this point, it is a conundrum that many star clusters distributed in a similar volume do not have large eccentricities (see also Fig. 2). We also point out that r_{90} , although a robust estimate of the star cluster size, does not represent the cluster Jacobi radius, which should strictly speaking be considered for monitoring any change in the star cluster dimension with the deprojected distance. Typical errors in r_{90} are $\sim 30\%$.

The mass versus age diagram of SMC star clusters depicted in Fig. 4 shows that those with eccentricities larger than ~ 0.4 are less massive than $\log(M/M_{\odot}) \sim 4.0$. More massive star clusters have eccentricities smaller than ~ 0.4 and seem to be among the oldest objects. We note however that not every old star cluster is more massive than $\log(M/M_{\odot}) \sim 4.0$. Likewise, we wonder on the presence of many star clusters less massive than $\log(M/M_{\odot}) \sim 4.0$ with eccentricities smaller than ~ 0.4 . Some aspects worthy of consideration to find an explanation, although beyond the scope of the present data sets, could be the existence of families of star clusters with different rotation velocities, or a differential perturbation by the LMC during the last close passage to the SMC (Patel et al. 2020).

Figure 4 also shows that the cluster mass distribution as a function of age is quite different from that of Milky Way open clusters located in a circle of radius 1.8 kpc from the Sun (Joshi et al. 2016, solid line). In the case of these open clusters, we can assume that the mass variation as a function of their ages is mainly caused by evolutionary effects, if the Milky Way gravitation field does not affect differently them in that relatively small circle. Furthermore, we can imagine straight lines parallel to that for Joshi et al. (2016)’s open clusters that correspond to star clusters under different tidal disruption regimes (Piatti et al. 2019), with those for weaker tidal fields located upward. Figure 4 shows a large number of SMC clusters that would seem to follow a similar trend, shifted by

$\Delta(\log(M/M_{\odot})) \sim 0.7$ (dashed line) toward larger masses. This nearly constant log mass difference could reflect the much stronger tidal field of the Milky Way at the solar circle in comparison with that of the SMC, assumed that the SMC star clusters are affected by the same SMC tidal field strength. We note that such a trend is followed by star clusters with some hundred Myr, for which mass loss is mainly driven by stellar evolution, and also for some older star clusters, where two-body relaxation can have a more important role. Star clusters older than ~ 1 Gyr practically did not survive along the dashed line. However, if more massive star clusters had experienced mass loss by tidal disruption as those along the dashed line, some of them would have been seen populating the region around the dashed line ($\log(\text{age}/\text{yr}) \gtrsim 9.3$). The fact that old clusters appear above the dashed line could be interpreted as they are affected by weaker gravitational field strengths. We note that most of them have eccentricities $\lesssim 0.4$, and are located at deprojected distances $\gtrsim 7$ -8 kpc. The observed mass range at any age is $\Delta(\log(M/M_{\odot})) \sim 2.0$.

4. Concluding remarks

We made use of available data sets of structural properties for a statistically significant sample of SMC star clusters with the aim of studying at what extend the SMC gravitational field are responsible of the star cluster shapes and sizes. Recently, it was shown the observed dependence of the core, half-mass, and Jacobi radii, alongside relaxation time, cluster mass loss by tidal disruption, among others, with the position in the galaxy of old globular Milky Way and LMC clusters. Although the SMC does not harbor star clusters as old as the ancient globular clusters, the spatial coverage of star clusters spanning the whole age range allows us to probe for tidal effects. Hill & Zaritsky (2006) performed an analysis of some structural properties of SMC star clusters. As far as we are aware, this is the first time that star cluster properties are analyzed in the context of the 3D geometry of the SMC.

We adopted an ellipsoid as a representation of the SMC with the three axes having different extensions. They have been adjusted combining the known star cluster age gradient and the recently SMC depth estimated from Classical Cepheids, RR Lyrae stars, and late-type eclipsing binaries. In this framework, each age is assigned to a unique ellipsoid. Therefore, by using the age of the star clusters and their projected positions in the sky with respect to the SMC center, we estimated their deprojected distances, which we used as a proxy of the SMC gravitational field. The use of deprojected distances solved the spurious effect of considering a star cluster to be located close to the SMC center, from its projected position in the sky.

We sought any trend between the star cluster size (represented by the 90% light radius), the eccentricity, the mass and age with the deprojected distance. We did find that the size of the star clusters would not seem to be sensitive to changes in their positions in the galaxy, because star clusters spanning the entire observed range are found everywhere. We point out, however, that Jacobi radii would be appropriate for a more definitive answer. The star cluster eccentricities reveal that those more elongated objects ($\epsilon \gtrsim 0.4$) are preferentially located at deprojected distances $\lesssim 7$ -8

kpc. This finding could be a hint for differential tidal effects between star clusters located closer and farther from the SMC center. However, we found a numerous population of stars clusters distributed inside the same volume that look like less elongated ($\epsilon \lesssim 0.4$).

Star clusters with estimated masses larger than $\log(M/M_{\odot}) \sim 4.0$ have relatively small eccentricities ($\epsilon \lesssim 0.4$), are older than $\log(\text{age}/\text{yr}) \sim 9.0$, considering the uncertainties in their estimated masses, and are mostly located in the outermost regions of the SMC. We would like to remind that we initially assumed a dependence in deprojected distance and cluster mass on age. These features could favor an scenario of differential tidal effects. Likewise, there is a large number of star clusters located at deprojected distances $\lesssim 7\text{--}8$ kpc that mimic the linear cluster mass versus age relationship of Milky Way open clusters placed within a circle of radius 1.8 kpc from the Sun, with a zero point offset of 0.7 toward more massive star clusters. We interpret this shift as originating from different gravitational field strengths.

Acknowledgements. I thank the referee for the thorough reading of the manuscript and timely suggestions to improve it.

References

- Baumgardt, H. & Makino, J. 2003, MNRAS, 340, 227
- Bianchini, P., Renaud, F., Gieles, M., & Varri, A. L. 2015, MNRAS, 447, L40
- Bica, E., Westera, P., Kerber, L. d. O., et al. 2020, AJ, 159, 82
- Carpintero, D. D., Gómez, F. A., & Piatti, A. E. 2013, MNRAS, 435 [arXiv:1307.6231]
- Chen, C. W. & Chen, W. P. 2010, ApJ, 721, 1790
- Cioni, M.-R. L., Clementini, G., Girardi, L., et al. 2011, A&A, 527, A116
- Crowl, H. H., Sarajedini, A., Piatti, A. E., et al. 2001, AJ, 122, 220
- Czesla, S., Schröter, S., Schneider, C. P., et al. 2019, PyA: Python astronomy-related packages
- Deason, A. J., Erkal, D., Belokurov, V., et al. 2020, arXiv e-prints, arXiv:2010.13801
- Dias, B., Kerber, L., Barbuy, B., Bica, E., & Ortolani, S. 2016, A&A, 591, A11
- D’Onghia, E. & Lake, G. 2008, ApJ, 686, L61
- Gieles, M. & Baumgardt, H. 2008, MNRAS, 389, L28
- Gieles, M., Heggie, D. C., & Zhao, H. 2011, MNRAS, 413, 2509
- Gieles, M., Lamers, H. J. G. L. M., & Portegies Zwart, S. F. 2007, ApJ, 668, 268
- Gieles, M., Portegies Zwart, S. F., Baumgardt, H., et al. 2006, MNRAS, 371, 793
- Gieles, M. & Renaud, F. 2016, MNRAS, 463, L103
- Glatt, K., Grebel, E. K., Sabbi, E., et al. 2008, AJ, 136, 1703
- Gnedin, O. Y., Lee, H. M., & Ostriker, J. P. 1999, ApJ, 522, 935
- Graczyk, D., Pietrzynski, G., Thompson, I. B., et al. 2020, arXiv e-prints, arXiv:2010.08754
- Heggie, D. & Hut, P. 2003, The Gravitational Million-Body Problem: A Multidisciplinary Approach to Star Cluster Dynamics
- Hill, A. & Zaritsky, D. 2006, AJ, 131, 414
- Hurley, J. R. & Mackey, A. D. 2010, MNRAS, 408, 2353
- Joshi, Y. C., Dambis, A. K., Pandey, A. K., & Joshi, S. 2016, A&A, 593, A116
- Kontizas, E., Kontizas, M., Sedmak, G., & Smareglia, R. 1989, AJ, 98, 590
- Kruijssen, J. M. D. & Mieske, S. 2009, A&A, 500, 785
- Kruijssen, J. M. D., Pelupessy, F. I., Lamers, H. J. G. L. M., Portegies Zwart, S. F., & Icke, V. 2011, MNRAS, 414, 1339
- Lamers, H. J. G. L. M. & Gieles, M. 2006, A&A, 455, L17

- Lamers, H. J. G. L. M., Gieles, M., Bastian, N., et al. 2005, *A&A*, 441, 117
- Maia, F. F. S., Dias, B., Santos, J. F. C., et al. 2019, *MNRAS*, 484, 5702
- Maia, F. F. S., Piatti, A. E., & Santos, J. F. C. 2014, *MNRAS*, 437, 2005
- Moore, B., Ghigna, S., Governato, F., et al. 1999, *ApJ*, 524, L19
- Muraveva, T., Subramanian, S., Clementini, G., et al. 2018, *MNRAS*, 473, 3131
- Nidever, D. L., Olsen, K., Walker, A. R., et al. 2017, *AJ*, 154, 199
- Patel, E., Kallivayalil, N., Garavito-Camargo, N., et al. 2020, *ApJ*, 893, 121
- Piatti, A. E. 2019, *ApJ*, 882, 98
- Piatti, A. E. & Geisler, D. 2013, *AJ*, 145, 17
- Piatti, A. E. & Mackey, A. D. 2018, *MNRAS*, 478, 2164
- Piatti, A. E., Sarajedini, A., Geisler, D., Clark, D., & Seguel, J. 2007, *MNRAS*, 377, 300
- Piatti, A. E., Webb, J. J., & Carlberg, R. G. 2019, *MNRAS*, 489, 4367
- Ripepi, V., Cioni, M.-R. L., Moretti, M. I., et al. 2017, *MNRAS*, 472, 808
- Shukirgaliyev, B., Parmentier, G., Just, A., & Berczik, P. 2018, *ApJ*, 863, 171
- Stanimirović, S., Staveley-Smith, L., & Jones, P. A. 2004, *ApJ*, 604, 176
- Udalski, A., Szymański, M. K., & Szymański, G. 2015, *Acta Astron.*, 65, 1
- van der Marel, R. P. & Kallivayalil, N. 2014, *ApJ*, 781, 121
- Webb, J. J., Harris, W. E., Sills, A., & Hurley, J. R. 2013, *ApJ*, 764, 124
- Webb, J. J., Sills, A., Harris, W. E., & Hurley, J. R. 2014, *MNRAS*, 445, 1048
- Zaritsky, D., Harris, J., Thompson, I. B., Grebel, E. K., & Massey, P. 2002, *AJ*, 123, 855